Effect of Hot Isostatic Pressing on the Microstructure of Directionally Solidified Nickel Alloy After SLM

Borisov, Evgenii; Gracheva, Anna; Popovich, Vera; Popovich, Anatoly

DOI
10.1007/978-3-030-92381-5_27

Publication date
2022

Document Version
Final published version

Published in
TMS 2022 151st Annual Meeting and Exhibition Supplemental Proceedings

Effect of Hot Isostatic Pressing on the Microstructure of Directionally Solidified Nickel Alloy After SLM

Evgenii Borisov, Anna Gracheva, Vera Popovich, and Anatoly Popovich

Abstract The paper investigates the effect of hot isostatic pressing of single-crystal nickel-based alloy manufactured by selective laser melting (SLM) with a high-temperature substrate preheating. A study of the structure and phase composition of the material before and after treatment has been carried out. It was found that as a result of such treatment, the ratio and proportion of the strengthening phases change; however, due to slow cooling after treatment, the optimal ratio and shape of the inclusions are not fixed. In addition, the hardening particles are precipitated.

Keywords Selective laser melting · Single-crystal alloys · Powder metallurgy · Additive manufacturing

Introduction

The current level of additive technologies development allows them to be seen as an alternative to existing subtractive manufacturing methods and to be integrated more and more deeply into various applications [1–11]. However, selective laser melting (SLM) technology has not yet become fully implemented in industry. The study of the possibilities of this technology will provide a fuller understanding of the prospects and feasibility of its implementation in various technological processes and expand the scope of its possible application. Most of the scientific papers are mainly aimed at expanding the capabilities of additive technologies and the limits of their application [12–20]. Post-treatment methods also have a significant impact on the capabilities of additive technologies [21–23]. This article includes the results of an experiment aimed at studying the effect of hot isostatic pressing (HIP) on the structure and phase composition of a heat-resistant nickel-based superalloy produced

E. Borisov (✉) · A. Gracheva · V. Popovich · A. Popovich
Peter the Great St. Petersburg Polytechnic University, St. Petersburg, Russia
e-mail: evgenii.borisov@icloud.com

V. Popovich
Faculty of Mechanical, Maritime, and Materials Engineering, Delft University of Technology (TU Delft), Mekelweg 2, 2628 CD Delft, The Netherlands

TMS 2022 151st Annual Meeting & Exhibition Supplemental Proceedings,
The Minerals, Metals & Materials Series,
https://doi.org/10.1007/978-3-030-92381-5_27

by SLM. The SLM process produces a large number of micro-defects, which reduce the strength and load bearing capabilities. One possible solution to this problem is hot isostatic pressing, but this method of post-processing has a negative effect on the structure of the resulting products. Various HIP effects on single-crystal nickel-based alloy are reflected in this paper.

Experimental Methods

For the manufacture of test samples, a powder of a heat-resistant nickel alloy obtained by plasma atomization of a rotating electrode was used. Alloy features a three-phase system consisting of a nickel-based γ-solid solution with an FCC crystal lattice, dispersion precipitates of the reinforcing γ'-phase based on the Ni_3Al intermetallic and MC type carbides [24]. The chemical composition of the alloy is shown in Table 1.

Samples were manufactured by Aconity3D MIDI selective laser melting machine (Aconity3D GmbH, Germany). SLM parameters resulting in the absence of cracks were selected based on our previous study [24]. The machine is equipped with laser source with variable focal spot diameter with Gauss power distribution and a maximum power of 1000 watts. Moreover, machine is equipped with a module to enable operation with platform preheating up to 1200 °C.

Rectangular specimens manufactured from the nickel-based superalloy (the chemical composition is given in Table 1) were exposed to heat treatment.

The hot isostatic pressing of the specimens was carried out according to the conditions: heating up to 1200 °C, pressure 160 MPa, holding for 3 h, followed by furnace cooling (Fig. 1).

After hot isostatic pressing, specimens were cut and polished along the building direction (BD). To highlight the microstructure, specimens were etched with $CuSO_4$,

Table 1 Chemical composition of nickel alloy powder (wt.%)

Ni	Cr	Al	Mo	W	Co	Re	Ta	Nb	C	B
Balance	4.9	5.9	1.1	8.4	9.0	1.93	4.1	1.6	0.12	0.01

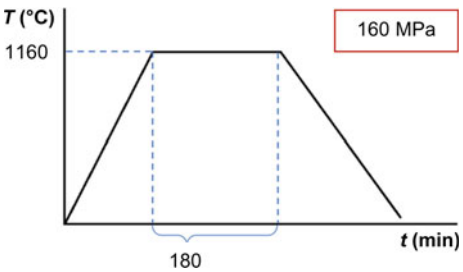

Fig. 1 Heat treatment parameters

H_2SO_4, and HCl. Carl Zeiss Supra 55VP scanning electron microscope was used for microstructure analysis. X-ray diffraction analysis was carried out using a diffractometer Bruker D8 Advance (CuKα = 0.15406 nm) in the 2θ-range of 30–100° with a scanning step of 0.020 and exposition of 1.5 s at every step. Structural parameters were refined by the Rietveld method; crystal density for equiatomic alloys was calculated from the mass and lattice parameter using the TOPAS5 program.

Results and Discussion

The microstructure of the obtained samples consists of elongated cells located mainly along the growing direction of the samples γ—solid solution with scattered particles γ'—phase formed on the basis of the intermetallic compound Ni_3Al (Fig. 2), which in turn consists of cuboid microparticles with an average size of ~200 nm (Fig. 2).

After selective laser melting, the structure of the samples is represented by grains elongated mainly in the direction of heat removal. The main phase is γ, with a distribution of inclusions of γ'—phase (Fig. 2). These inclusions are cuboids with an average size of about 0.2 μm.

Inclusions in the form of carbides of alloying elements (Nb and Mo) can be seen along the boundaries of the γ-phase cells. Such precipitates impede the movement of the grain boundaries of the base alloy matrix at high temperatures and prevent the appearance of plastic deformation (Fig. 3). The presence of such carbides, however, can lead to the formation of defects in the form of hot cracks and pores [24, 25].

The microstructure of the sample after hot isostatic pressing is shown in Fig. 4. It was found that the γ'—phase inclusions increased in size and changed their shape. At the same time, the total γ'—phase content in the alloy structure decreased.

Phase composition of the sample before (Figs. 4, 1) and after (Figs. 4, 2) hot isostatic pressing shows that all peaks belong to the HCC phase. The structure of the samples is characterized by a strong texture. The strong (110) peak of sample

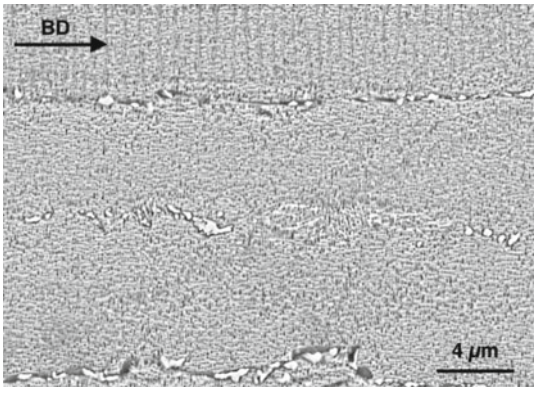

Fig. 2 SEM image of the γ/γ' microstructure after SLM

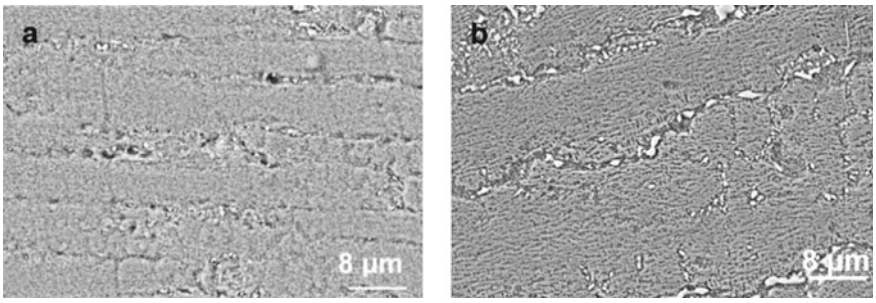

Fig. 3 SEM images of the γ/γ' microstructure: **a** after SLM; **b** after hot isostatic pressing

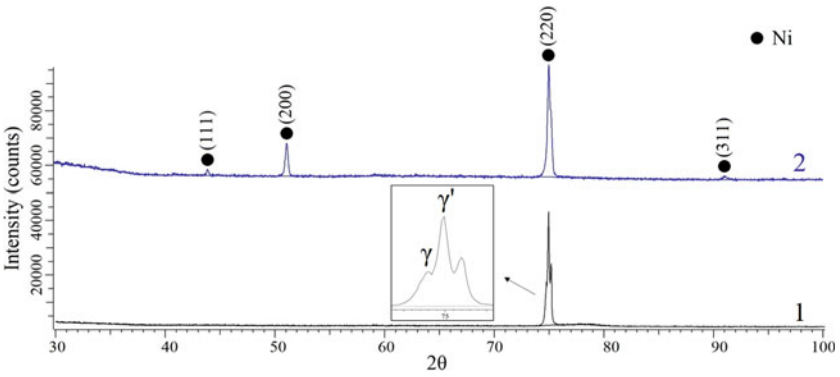

Fig. 4 XRD pattern of the nickel-based superalloy samples. 1-before HIP, 2-after HIP

1 indicates that the crystallites are preferably (110)-oriented along the surface. In sample 2, the orientation of crystallites along the direction perpendicular to the (110) plane is observed, and the March-Dallas coefficient was 0.21. The detailed diffractogram of the sample examined before heat treatment shows that the separation of the γ and γ' phases is observed in the region of 75°. The crystal lattice parameter of the γ-phase is $a = 0.3589$ nm, and the γ'-phase is $a = 0.3579$ nm. The misfit value $\Delta a = (a\text{y} - a\text{y}')/\text{ay}'$ for the sample before heat treatment was 0.003.

In the second sample, reflexes from all planes are visible after the hot isostatic pressing, which may be due to recrystallization of grains in the places of defects (cracks) in the process of hot isostatic pressing in the sample.

In the samples after hot isostatic pressing, in contrast to the initial samples, there is no peak separation. This effect can be caused due to a decrease in the lattice parameter of the gamma of the solid solution, which is caused by the release of carbides of elements Ta, W, etc. Thus, a decrease in the volume fraction of γ'—phase cells can be associated with a change in the crystal lattice parameter and a change in the chemical composition of the phases.

Conclusions

The effect of hot isostatic pressing of a heat-resistant nickel alloy samples fabricated by selective laser melting on the structure and phase composition was investigated. It was found that during hot isostatic pressing, the proportion of the gamma prime phase in the alloy structure decreases. In addition, inclusions change their shape and increase in size. This may be caused by a change in the period of the crystal lattice of the matrix γ—phase, which occurs due to the precipitation of carbides of alloying elements. This alignment can occur due to the release of carbides TaC and WC and, as a consequence, depletion of the γ—solid solution with alloying elements Ta and W, which to the greatest extent increases the lattice period of the γ—solid solution. Local recrystallization is also observed after hot isostatic pressing. Such recrystallization can occur in the areas of micropores and cracks in the process of their closure.

Acknowledgements This research was supported by Russian Science Foundation grant (project No. 19-79-30002).

References

1. Kozlova EV, Yakinchuk VV, Starikov KA et al (2021) Life cycle management of the 3D-printer technology to design an underwater drone hull to study the arctic. IOP Conf Ser Earth Environ Sci 625:012016. https://doi.org/10.1088/1755-1315/625/1/012016
2. Kozlova EV, Starikov KA, Konakhina NA, Aladyshkin IV (2020) Usage of additive technologies in the Arctic region. IOP Conf Ser Earth Environ Sci 539:012140. https://doi.org/10.1088/1755-1315/539/1/012140
3. Sotov A, Kantyukov A, Popovich A, Sufiiarov V (2021) LCD-SLA 3D printing of BaTiO3 piezoelectric ceramics. Ceramics Int 47(21):30358–30366
4. Ekaterina Kozlova ND (2021) The impact of technological development factors on the quality of life: a comparative analysis OF E7 and G7. Int J Qual Res 16:03. https://doi.org/10.24874/IJQR16.02-18
5. Javaid M, Haleem A (2018) Additive manufacturing applications in orthopaedics: a review. J Clin Orthop Trauma 9:202–206. https://doi.org/10.1016/j.jcot.2018.04.008
6. Salmi M (2021) Additive manufacturing processes in medical applications. Materials (Basel) 14:191. https://doi.org/10.3390/ma14010191
7. Javaid M, Haleem A (2018) Additive manufacturing applications in medical cases: a literature based review. Alexandria J Med 54:411–422. https://doi.org/10.1016/j.ajme.2017.09.003
8. Patel P, Gohil P (2021) Role of additive manufacturing in medical application COVID-19 scenario: India case study. J Manuf Syst 60:811–822. https://doi.org/10.1016/j.jmsy.2020.11.006
9. Otero JJ, Vijverman A, Mommaerts MY (2017) Use of fused deposit modeling for additive manufacturing in hospital facilities: European certification directives. J Cranio-Maxillofacial Surg 45:1542–1546. https://doi.org/10.1016/j.jcms.2017.06.018
10. Sacco E, Moon SK (2019) Additive manufacturing for space: status and promises. Int J Adv Manuf Technol 105:4123–4146. https://doi.org/10.1007/s00170-019-03786-z
11. Farré-Guasch E, Wolff J, Helder MN et al (2015) Application of additive manufacturing in oral and maxillofacial surgery. J Oral Maxillofac Surg 73:2408–2418. https://doi.org/10.1016/j.joms.2015.04.019

12. Sufiiarov V, Kantyukov A, Polozov I (2020) Reaction sintering of metal-ceramic AlSi-Al2O3 composites manufactured by binder jetting additive manufacturing process, pp 1148–1155
13. Polozov I, Sufiiarov V, Kantyukov A et al (2020) Microstructure, densification, and mechanical properties of titanium intermetallic alloy manufactured by laser powder bed fusion additive manufacturing with high-temperature preheating using gas atomized and mechanically alloyed plasma spheroidized powder. Addit Manuf 34:101374. https://doi.org/10.1016/j.addma.2020.101374
14. Maximov M, Nazarov D, Rumyantsev A et al (2020) Atomic layer deposition of lithium–nickel–silicon oxide cathode material for thin-film lithium-ion batteries. Energies 13:2345. https://doi.org/10.3390/en13092345
15. Popovich AA, Masaylo DV, Sufiiarov VS et al (2016) A laser ultrasonic technique for studying the properties of products manufactured by additive technologies. Russ J Nondestruct Test 52:303–309. https://doi.org/10.1134/S1061830916060097
16. Novikov PA, Kim AE, Ozerskoi NE et al (2019) Plasma chemical synthesis of aluminum nitride nanopowder. Key Eng Mater 822:628–633. https://doi.org/10.4028/www.scientific.net/KEM.822.628
17. Polozov I, Sufiiarov V, Starikov K, Popovich A (2021) In situ synthesized Ti2AlNb-based composites produced by selective laser melting by addition of SiC-whiskers. Mater Lett 297:129956. https://doi.org/10.1016/j.matlet.2021.129956
18. Sufiiarov V, Kantyukov A, Popovich A, Sotov A (2021) Structure and properties of barium titanate lead-free piezoceramic manufactured by binder jetting process. Materials (Basel) 14:4419. https://doi.org/10.3390/ma14164419
19. Borisov EV, Popovich VA, Popovich AA et al (2020) Selective laser melting of Inconel 718 under high laser power. Mater Today Proc 30:784–788. https://doi.org/10.1016/j.matpr.2020.01.571
20. Polozov I, Starikov K, Popovich A, Sufiiarov V (2021) Mitigating inhomogeneity and tailoring the microstructure of selective laser melted titanium orthorhombic alloy by heat treatment, hot isostatic pressing, and multiple laser exposures. Materials (Basel) 14:4946. https://doi.org/10.3390/ma14174946
21. Polozov I, Sufiiarov V, Kantyukov A, Popovich A (2019) Selective Laser Melting of Ti2AlNb-based intermetallic alloy using elemental powders: effect of process parameters and post-treatment on microstructure, composition, and properties. Intermetallics 112:106554. https://doi.org/10.1016/j.intermet.2019.106554
22. Sufiiarov VS, Popovich AA, Borisov EV, Polozov IA (2017) Evolution of structure and properties of heat-resistant nickel alloy after selective laser melting, hot isostatic pressing and heat treatment. Tsvetnye Met 77:77–82
23. Popovich VA, Borisov EV, Sufiyarov VS et al (2019) Tailoring the properties in functionally graded alloy inconel 718 using additive technologies. Met Sci Heat Treat 60:701–709. https://doi.org/10.1007/s11041-019-00343-z
24. Borisov E, Starikov K, Popovich A, Popovich V (2020) CRACKs formation in nickel-based single crystal alloy manufactured by selective laser melting, pp 875–879
25. Evgenii B, Kirill S, Anatoly P, Vera P (2021) Melt pool evolution in high-power selective laser melting of nickel-based alloy, pp 142–148